NJC

Accepted Manuscript

This is an *Accepted Manuscript*, which has been through the Royal Society of Chemistry peer review process and has been accepted for publication.

Accepted Manuscripts are published online shortly after acceptance, before technical editing, formatting and proof reading. Using this free service, authors can make their results available to the community, in citable form, before we publish the edited article. We will replace this *Accepted Manuscript* with the edited and formatted *Advance Article* as soon as it is available.

You can find more information about *Accepted Manuscripts* in the Information for Authors.

Please note that technical editing may introduce minor changes to the text and/or graphics, which may alter content. The journal's standard Terms & Conditions and the Ethical guidelines still apply. In no event shall the Royal Society of Chemistry be held responsible for any errors or omissions in this *Accepted Manuscript* or any consequences arising from the use of any information it contains.

ROYAL SOCIETY OF CHEMISTRY

www.rsc.org/njc

Journal Name

ARTICLE

Tunable blue-green emitting and energy transfer of Eu^{2+}/Tb^{3+} codoped $Sr_3La(PO_4)_3$ phosphor for near-UV white LEDs

Received 00th January 20xx,
Accepted 00th January 20xx

DOI: 10.1039/x0xx00000x

www.rsc.org/

Qiongyu Bai, Zhijun Wang*, Panlai Li*, Shuchao Xu, Ting Li, Zhiping Yang

A series of Eu^{2+} and Tb^{3+} doped $Sr_3La(PO_4)_3$ phosphors have been synthesized via the high-temperature solid-state reaction method. X-ray diffraction (XRD) patterns, luminescence spectra including temperature-dependent luminescence spectra, and fluorescence decay lifetimes have been used to characterize the as-prepared samples. Under ultraviolet excitation, $Sr_3La(PO_4)_3:Eu^{2+}$ shows a strong blue emission around 418 nm and a shoulder centered at 500 nm, which based on the substitution of two kinds of Sr^{2+} sites by Eu^{2+} ions (Eu1 and Eu2). $Sr_3La(PO_4)_3:Tb^{3+}$ shows characteristic emission lines of Tb^{3+} under 376 nm excitation. For $Sr_3La(PO_4)_3:Eu^{2+}$, Tb^{3+} phosphor, the similar excitation spectra monitored at 418, 500 and 545 nm have been observed, which illustrates the possibility of energy transfer from Eu^{2+} to Tb^{3+} ions. Compared with the Tb^{3+} singly doped phosphor, the codoped phosphors have more intense absorption in the n-UV range and stronger emission of the Tb^{3+} ions, which are attributed to the effective energy transfer from the Eu^{2+} to Tb^{3+} ions. The variations in the emission spectra, emission color and decay lifetimes further demonstrate the existence of energy transfer from Eu^{2+} to Tb^{3+} ions under ultraviolet excitation. For Eu1 and Eu2, the energy transfer mechanism has been confirmed to be quadrupole-quadrupole and dipole-quadrupole interaction, respectively. The results which can be validated via the agreement of critical distances obtained from the concentration quenching (21.62 Å). These results show that the phosphors may possess potential applications in ultraviolet-based white light-emitting diodes.

1 Introduction

White light emitting diodes (LEDs) are mainstream in solid-state lighting because of several advantages, such as energy saving, no mercury pollution, long life, short response time, small size and high energy efficiency.[1] The conventional method to create white LEDs is the combination of a blue LED and a yellow-emitting phosphor YAG:Ce^{3+}, and the white LEDs have a high efficiency (>100 lm/W). However, the white LEDs exhibit a poor color rendering index (CRI≈70-80) and a high correlated color temperature (CCT≈7750 K) because of lacking the red component.[2] In order to achieve white light with the high CRI and suitable CCT, the alternative way is the combination of an ultraviolet (UV) or near UV (n-UV) LED with the tri-color phosphors. Therefore, the excellent tri-color phosphors play an important role in the development of white LEDs.[3-5]

It is well known that Tb^{3+} ion is frequently used as an activator of the green luminescent materials due to its predominant $^5D_4$-$^7F_5$ transition peak around 545 nm.[6] The major problem for the Tb^{3+} ion is the lack of efficient and broad excitation band from n-UV to visible region, which limits its application in n-UV white LEDs.[6] Since the f-f transition is spin-forbidden, the emission intensity of the Tb^{3+} ion is weak. An efficacious way to solve this problem is by utilizing energy transfer from sensitizers to activators in proper host.[7-12] As is well known, Eu^{2+} is of great interest for application because d-f emission is partly allowed, resulting in high emission intensity.[13] Emission energy shows a strong dependence on crystal field and covalence, and Eu^{2+} doped samples usually have a strong absorption in the region from UV to visible region and exhibit broad emission band covering the color from blue to red.[14-17] Therefore, in many compounds, the energy transfer from Eu^{2+} to activators has been investigated.[18-22] For example, the efficient energy transfer takes place between Eu^{2+} and Mn^{2+} in $NaScSi_2O_6$, leading to a series of color-tunable phosphors emitting at 533 and 654 nm for the $NaScSi_2O_6:Eu^{2+}$, Mn^{2+} phosphors under excitation at 365 nm;[23] For $Ba_{1.55}Ca_{0.45}SiO_4:Eu^{2+}$,$Mn^{2+}$ phosphor, the energy-transfer efficiency between Eu^{2+} and Mn^{2+} increases and tunable emission can be got with an increase of the Mn^{2+} content.[24] Since the Eu^{2+} ion may be a good sensitizer for Tb^{3+} ion, it is important to study the luminescent properties of Eu^{2+} and Tb^{3+} codoped phosphors.

Generally, the phosphors consist of activator and host, where the choice of host is considered as the key factor for obtaining efficient emission. Recently, Eulytite-type orthophosphates with the general formula $M_3^IM^{II}(PO_4)_3$ (M^I=Ca, Sr, Ba and Pb; M^{II}=La, Y, Sc, Bi, Tb and

College of Physics Science & Technology, Hebei Key Lab of Optic-Electronic Information and Materials, Hebei University, Baoding 071002, China
† li_panlai@126.com; wangzj1998@126.com.
Electronic Supplementary Information (ESI) available: [details of any supplementary information available should be included here]. See DOI: 10.1039/x0xx00000x

In) have attracted extensive attention as host compounds for lanthanide activators because of the excellent thermal stability and optical property.[25-28] For example, the researchers have reported the luminescent properties and energy transfer of Eu^{2+} and Mn^{2+} in $Ba_3Gd(PO_4)_3$, $Sr_3Sc(PO_4)_3$ and $Sr_3Y(PO_4)_3$.[29-31] Our previous work has described that the allowed $4f^5d^1$-$4f^7$ electric dipole transition of Eu^{2+} ions in the $Sr_3La(PO_4)_3$ can emit blue light, and there is the spectral overlap between the emission spectra of Eu^{2+} and characteristics excitation of Tb^{3+} in $Sr_3La(PO_4)_3$.[9, 32] Thus Eu^{2+} ion may transfer its energy to Tb^{3+} ion, and enhance its emission intensity of Tb^{3+} in $Sr_3La(PO_4)_3$. In the present work, the fluorescence decay curves are fitted and analyzed, the luminescent properties and energy transfer mechanism of $Sr_3La(PO_4)_3$:Eu^{2+}, Tb^{3+} phosphors are investigated in detail. As a tunable blue-green emitting phosphor, $Sr_3La(PO_4)_3$:Eu^{2+}, Tb^{3+} may be a potential applications in UV-based white LEDs.

2 Experimental

2 Samples preparation

$SrCO_3$ (Analytical Reagent, A. R.), $NH_4H_2PO_4$ (A. R.), La_2O_3 (A. R.), Tb_4O_7 (99.99%) and Eu_2O_3 (99.99%) were used as the raw materials. A series of $Sr_{3-x}La_{1-y}(PO_4)_3$:xEu^{2+}, yTb^{3+} (x and y, molar concentration) phosphors were synthesized by a high temperature solid-state method. The stoichiometric amount of raw materials was thoroughly mixed and ground by an agate mortar and pestle for more than 30 min till they are uniformly distributed. Then the grinded powder is heated at 1300 ^oC for 3 h in crucibles along with the reducing agent (a mixture of 5% H_2 and 95% N_2). Finally, the samples are cooled to room temperature and ground them into power for measurements.

2.2 Materials characterization

Phase formation of phosphors is carefully checked by powder X-ray diffraction (XRD) analysis (Bruker AXS D8 advanced automatic diffractometer (Bruker Co., German)), with Ni-filtered Cu Kα1 radiation (λ=0.15405 nm) operating at 40 kV and 40 mA, and a scan rate of 0.02°/s is applied to record the patterns in the 2θ range from 10° to 70°. The photoluminescence spectra and luminescence decay curves are detected by a FLS920 fluorescence spectrometer, the scanning wavelength range from 200 to 700 nm, a spectral resolution of 0.2 nm, and the exciting sources are a 450 W Xe lamp and a 320-picosecond pulsed diode laser. Photoluminescence absolute quantum efficiency (QE) was measured by an absolute photoluminescence quantum yield measurement system (HORIBA, FL-1057). Commission International de l'Eclairage (CIE) chromaticity coordinates of sample are measured by a PMS-80 spectra analysis system. All measurements are carried out at room temperature. High-temperature photoluminescence spectra are detected by a fluorescence spectrophotometer (Hitachi F-4600) with a TAP-02 high temperature control system, the scanning wavelength range from 400 to 700 nm, a spectral resolution of 0.2 nm, and the exciting source is a 450 W Xe lamp.

3 Results and discussion

3.1 Phase formation

The XRD patterns of $Sr_{3-x}La_{1-y}(PO_4)_3$:xEu^{2+}, yTb^{3+} are measured, and the similar diffraction patterns are observed for each sample. As a representative, we only select the results of $Sr_{2.97}La(PO_4)_3$:$0.03Eu^{2+}$, $Sr_3La_{0.93}(PO_4)_3$:$0.07Tb^{3+}$ and $Sr_{2.97}La_{0.93}(PO_4)_3$:$0.03Eu^{2+}$, $0.07Tb^{3+}$. Figure 1 shows all the diffraction peaks match well with that of the cubic $Sr_3La(PO_4)_3$ according to the standard reference of ICSD card no.69432, and no traces of other phases are observed. Considering the ionic radii and valence state of Eu^{2+}/Sr^{2+} and Tb^{3+}/La^{3+} ions, we suppose that the Eu^{2+} and Tb^{3+} ions occupy the Sr^{2+} and La^{3+} sites, respectively. The crystal structures of the eulytite-type materials $M_3^IM^{II}(PO_4)_3$ are well known to be cubic (space group number 220) and isomorphous with eulytine mineral ($Bi_4Si_3O_{12}$). The $Sr_3La(PO_4)_3$ structure is described in the cubic I-43d space group with lattice constant a=10.192Å, and Sr and La occupy the same site with a C_3 symmetry. According to Ref [33], the general feature of $Sr_3La(PO_4)_3$ structure could be regarded as a three-dimensional packing of $[PO_4]^{3-}$ anionic tetrahedra and La/Sr octahedra, arranged in a manner to share common apices. It is interesting that all the $[PO_4]^{3-}$ tetrahedral are totally independent while the La/Sr octahedra share edges with each other and form a three-dimensional network.

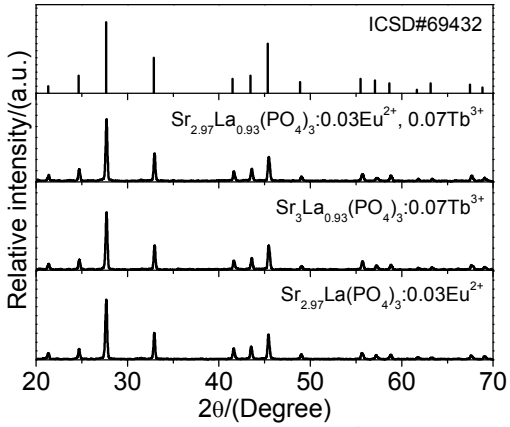

Figure 1. XRD patterns of $Sr_{2.97}La(PO_4)_3$:$0.03Eu^{2+}$, $Sr_3La_{0.93}(PO_4)_3$:$0.07Tb^{3+}$ and $Sr_{2.97}La_{0.93}(PO_4)_3$:$0.03Eu^{2+}$, $0.07Tb^{3+}$.
Standard data of $Sr_3La(PO_4)_3$ (ICSD No. 69432) is shown as reference.

3.2 Luminescence properties of $Sr_3La(PO_4)_3$:Eu^{2+} and $Sr_3La(PO_4)_3$:Tb^{3+}

According to our previous results,[32] the Eu^{2+} ions can enter the structure at two distinct Sr^{2+} sites in the $Sr_3La(PO_4)_3$. The blue

emission (Eu1) is due to nine-coordinated Eu^{2+} luminescence center and the cyan emission (Eu2) is attributed to six-coordinated Eu^{2+} luminescence center. Moreover, when Eu^{2+} concentration is rather low, despite the emission spectrum shows two emission peaks, however, the cyan emission is stronger than that of blue emission. As increasing the Eu^{2+} concentration, the blue emission gradually increases, but the cyan emission decreases. When the Eu^{2+} concentration (*x*) is 0.03, there is no the obvious cyan emission characteristic; however, the blue emission intensities reach the maximum, then, the blue emission intensity decreases with increasing Eu^{2+} concentration, viz., the optimal Eu^{2+} concentration (*x*) is 0.03. Moreover, our group reported the luminescent properties of $Sr_{3-x}La(PO_4)_3:xEu^{2+}$ with different Eu^{2+} concentration. Therefore, in this work, in order to investigate the luminescence and energy transfer of Eu^{2+}/Tb^{3+} codoped $Sr_3La(PO_4)_3$, we only selected $Sr_3La(PO_4)_3:0.03Eu^{2+}$ as the research object.

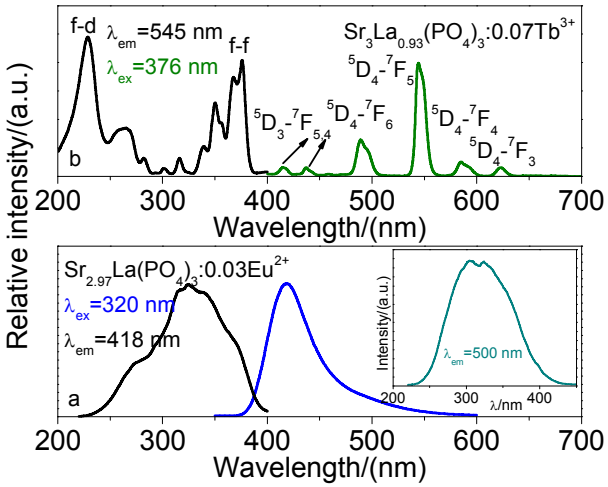

Figure 2. Emission and excitation spectra of $Sr_{2.97}La(PO_4)_3:0.03Eu^{2+}$ (λ_{ex}=320 nm, λ_{em}=418 nm) (a), $Sr_3La_{0.93}(PO_4)_3:0.07Tb^{3+}$ (λ_{ex}=376 nm, λ_{em}=545 nm) (b). Inset of Figure 2a: Excitation spectra of $Sr_{2.97}La(PO_4)_3:0.03Eu^{2+}$ (λ_{em}=500 nm).

Figure 2 depicts the luminescent properties of $Sr_3La(PO_4)_3:0.03Eu^{2+}$ and $Sr_3La(PO_4)_3:0.07Tb^{3+}$. As shown in Figure 2a, when excited at 320 nm, $Sr_3La(PO_4)_3:0.03Eu^{2+}$ shows a strong blue emission around 418 nm and a shoulder locating at 500 nm. Both the intense broad peaks are originated from 5d→4f transition of Eu^{2+} ions. Monitored at 418 nm, the excitation spectrum exhibits a broad band in the range from 220 to 400 nm, which is assigned to the transitions between the ground state $4f^7$ and the crystal-field split $4f^65d$ configuration. For the 500 nm emission, the inset of Figure 2a presents the corresponding excitation, and it also shows a broad band in the range from 220 to 450 nm.

When tuned the Tb^{3+} concentration (y) from 0.001 to 0.10, there is no the concentration quenching of Tb^{3+} in $Sr_3La(PO_4)_3$ in our experiment, and the inset of Figure S1b shows the relative intensity of $Sr_3La(PO_4)_3:Tb^{3+}$ with different Tb^{3+} concentration. In this section, we freely chose $Sr_3La(PO_4)_3:0.07Tb^{3+}$ as research object. Figure2b presents the emission and excitation spectra of $Sr_3La(PO_4)_3:0.07Tb^{3+}$. The excitation spectrum of $Sr_3La(PO_4)_3:Tb^{3+}$ presents a broad band from 200 to 250 nm with a maximum at 229 nm and some transitions from 250 to 400 nm. The former is related to the $4f^8$-$4f^75d$ transition of Tb^{3+}, and the latter is ascribed to its intra-(4f) transitions. Under the 376 nm excitation, $Sr_3La(PO_4)_3:Tb^{3+}$ can emit green light, and the obtained emission spectrum consists of the f-f transition lines within the Tb^{3+} $4f^8$ electron configuration, that is, $^5D_3$→$^7F_5$ (415 nm), $^5D_3$→$^7F_4$ (437 nm), $^5D_4$→$^7F_6$ (489 nm), $^5D_4$→$^7F_5$ (545 nm), $^5D_4$→$^7F_4$ (585 nm) and $^5D_4$→$^7F_3$ (622 nm).

3.3 Luminescence and energy transfer of $Sr_3La(PO_4)_3:Eu^{2+}$, Tb^{3+}

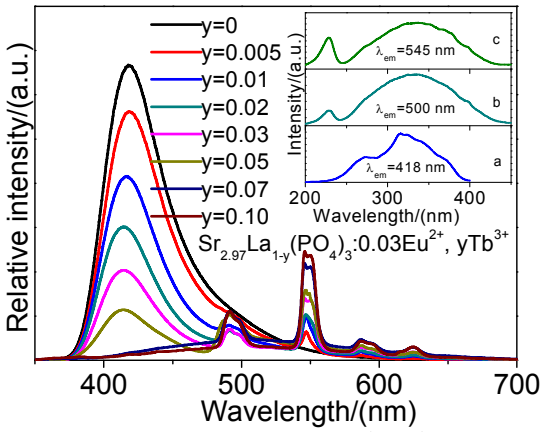

Figure 3. Emission spectra of $Sr_{2.97}La_{1-y}(PO_4)_3:0.03Eu^{2+}$, yTb^{3+} (*y*=0-0.10) (λ_{ex}=320 nm). Inset: Excitation spectra (λ_{em}=418 nm) (a), (λ_{em}=500 nm) (b) and (λ_{em}=545 nm) (c).

As shown in Figure S1, because there has obvious overlap between the emission band of Eu^{2+} and excitation band of Tb^{3+} in the range of 370-500 nm. Therefore, the Eu^{2+} ion (Eu1 and Eu2) may transfer its energy to Tb^{3+} ion in $Sr_3La(PO_4)_3$. Under the 320 nm excitation of Eu^{2+}, the emission spectra of $Sr_3La(PO_4)_3:0.03Eu^{2+}$, yTb^{3+} (*y*=0-0.10) are measured and shown in Figure 3. There are both Eu^{2+} and Tb^{3+} emission bands, and the emission intensities of Eu^{2+} decrease with increase the Tb^{3+} concentration, which can confirm the existence of energy transfer from Eu^{2+} to Tb^{3+} in $Sr_3La(PO_4)_3$. In order to study the energy transfer from Eu^{2+} to Tb^{3+}, the normalized intensities of Eu^{2+} and Tb^{3+} in $Sr_3La(PO_4)_3$ are recorded and shown in Figure S2. It shows that the emission intensities of Eu^{2+} obviously decrease, and that of Tb^{3+} gradually increase with increase the Tb^{3+} concentration. As shown in the inset (a), for the 418 nm, the excitation spectrum presents the characteristics excitation band of Eu1. However, For 500 nm (b, Eu2) and 545 nm (c, Tb^{3+}), the corresponding excitation

spectra generally depict the excitation characteristics of Eu^{2+}, moreover, in the range of 200-250 nm, there is the $4f^8$-$4f^7$5d transition of Tb^{3+}. The results obviously demonstrate that the energy transfer from Eu^{2+} to Tb^{3+} is effective.

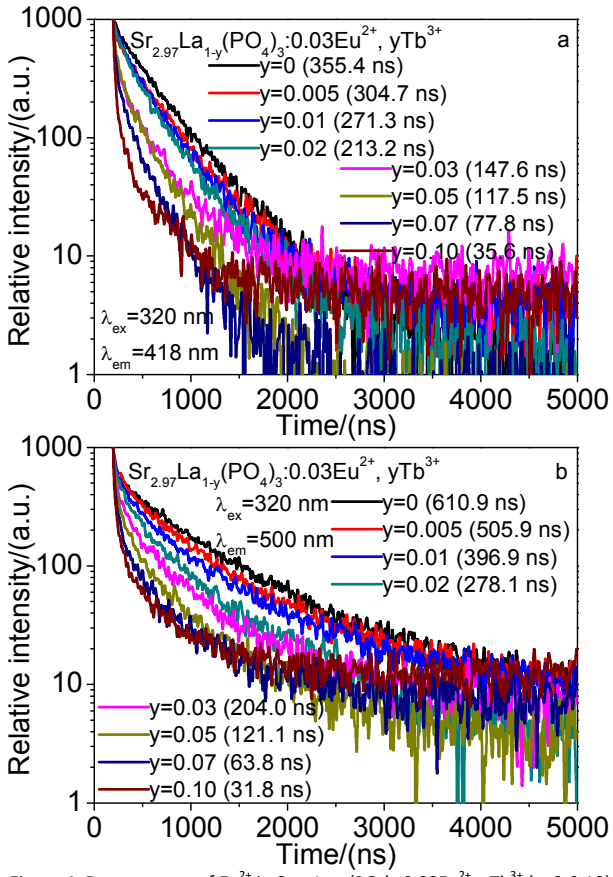

Figure 4. Decay curves of Eu^{2+} in $Sr_{2.97}La_{1-y}(PO_4)_3$:0.03$Eu^{2+}$, $y$$Tb^{3+}$ (y=0-0.10) (a, Eu1) and (b, Eu2) (λ_{ex}=320 nm) with different Tb^{3+} concentration.

To further validate the energy transfer from Eu^{2+} to Tb^{3+}, we investigated the lifetimes of Eu^{2+}. The decay curves of $Sr_3La(PO_4)_3$:0.03Eu^{2+}, $y$$Tb^{3+}$ (y=0-0.10) excited at 320 nm and monitored at 418 nm (Eu1) and 500 nm (Eu2) are shown in Figure 4a and 4b, respectively. The decay curves are well fitted with a second-order exponential decay mode by the Eq.1[34]

$$I=A_1\exp(-t/\tau_1)+A_2\exp(-t/\tau_2) \quad (1)$$

where I is the luminescence intensity; A_1 and A_2 are constants; t is the time, and τ_1 and τ_2 are the lifetimes for the rapid and slow decays, respectively. The average lifetimes (τ*) can be calculated by the formula as follow[34]

$$\tau^*=(A_1\tau_1^2+A_2\tau_2^2)/(A_1\tau_1+A_2\tau_2) \quad (2)$$

For 418 nm emission (Eu1) and 500 nm emission (Eu2), the calculated average lifetimes (τ*) are shown in Figure 4a and 4b, respectively.

$$\eta_T=1-(I_S/I_{S0}) \quad (3)$$

Generally, the energy transfer efficiency (η_T) from a sensitizer to an activator can also be expressed by equation 3, which is extensively used in the Eu^{2+}/Mn^{2+} and Ce^{3+}/Tb^{3+} co-doped phosphors,[7-9, 29-31] where I_{S0} and I_S are the luminescent intensities of the sensitizer in the absence and presence of the activator. Actually, the energy transfer efficiency can also be calculated using the following equation by Paulose et al.[35]

$$\eta_T=1-(\tau_S/\tau_{S0}) \quad (4)$$

where τ_{S0} and τ_S are the decay lifetimes of the sensitizer Eu^{2+} in the absence and presence of the activator Tb^{3+}. According to the calculated average lifetimes (τ*), the energy transfer efficiency (η_T) is achieved and shown in Figure 5. The results show that the energy transfer efficiency from Eu^{2+} to Tb^{3+} gradually increases with increase Tb^{3+} concentration. For instance, at y=0.10, the energy transfer efficiencies (η_T) are observed as 89.98% (Eu1) and 94.80% (Eu2), respectively.

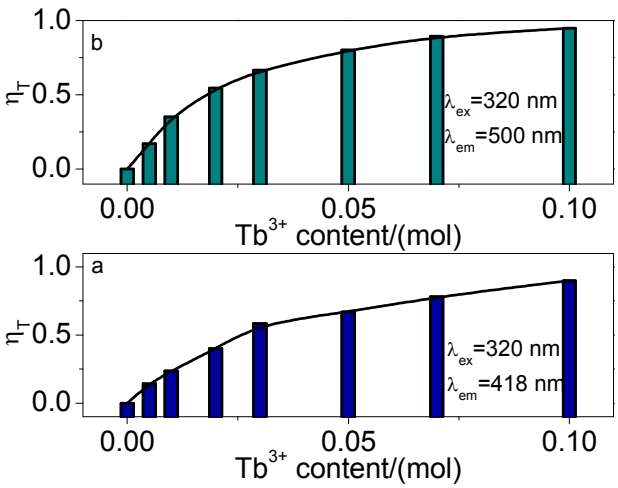

Figure 5. Energy transfer efficiencies (η_T) from Eu^{2+} to Tb^{3+} on concentrations in $Sr_{2.97}La_{1-y}(PO_4)_3$:0.03$Eu^{2+}$, $y$$Tb^{3+}$ (λ_{ex}=320 nm). (a), (λ_{em}=418 nm) (b) and (λ_{em}=500 nm)

In order to determine the energy transfer mechanism in $Sr_3La(PO_4)_3$:Eu^{2+}, Tb^{3+}, it is necessary to know the critical distance (R_c) between activators. With increasing Tb^{3+} concentration, the distance between Eu^{2+} ions and Tb^{3+} ions becomes shorter and shorter, thus the probability of energy migration increases. When the distance becomes small enough, the concentration quenching

occurs and the energy migration is hindered. The critical distance $R_{Eu\text{-}Tb}$ between Eu^{2+} and Tb^{3+} can be estimated by[36]

$$R_{Eu\text{-}Tb}=2[3V/(4\pi C_c N)]^{1/3} \quad (5)$$

where C is the sum concentration of Eu^{2+} and Tb^{3+}, N is the number of Z ions in the unit cell (for $Sr_3La(PO_4)_3$, N=4), and V is the volume of the unit cell (for $Sr_3La(PO_4)_3$:Eu^{2+}, Tb^{3+}, V=1058.7 Å^3). C_c is the sum concentration of Eu^{2+} and Tb^{3+} (C_c=0.05) at which the emission intensity of donor (Eu^{2+}) in the presence of acceptor (Tb^{3+}) is half of that in the absence of acceptor (Tb^{3+}).[37, 38] Using the parameters, $R_{Eu\text{-}Tb}$ of energy transfer is calculated to be about 21.62 Å. The value is much larger than the typical critical distance for the exchange interaction (5 Å).[36] Therefore, the results indicate that the exchange interaction plays no role in the energy transfer process for $Sr_3La(PO_4)_3$:Eu^{2+}, Tb^{3+}. Hence, the energy transfer between Eu^{2+} and Tb^{3+} exists in $Sr_3La(PO_4)_3$:Eu^{2+}, Tb^{3+}, and the emission intensities of Tb^{3+} are obviously enhanced by the efficient energy transfer from Eu^{2+} to Tb^{3+}, which belongs to the multipolar interaction.

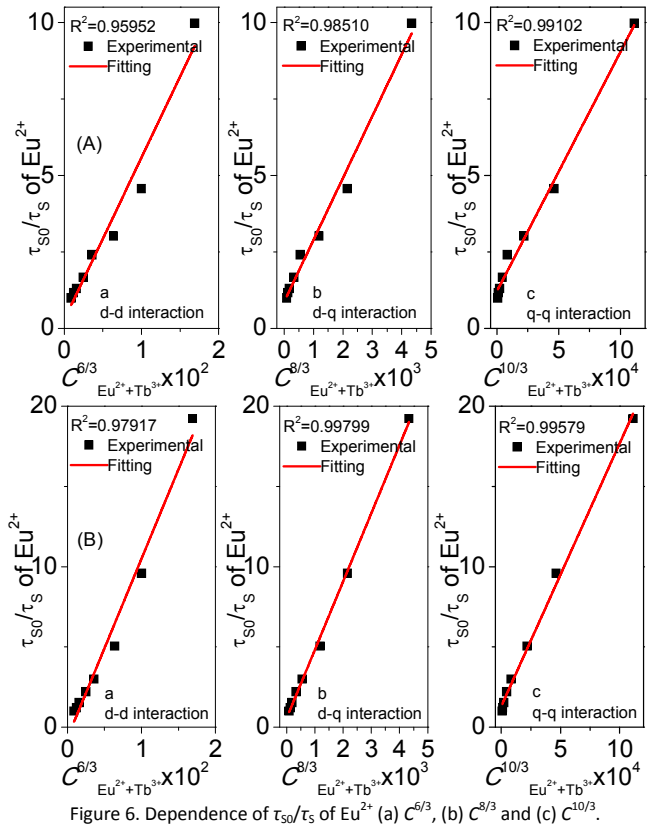

Figure 6. Dependence of τ_{S0}/τ_S of Eu^{2+} (a) $C^{6/3}$, (b) $C^{8/3}$ and (c) $C^{10/3}$. (A) Eu1 and (B) Eu2

On the basis of Dexter's energy transfer formula for multipolar interactions, the following relation can be obtained[39]

$$(\eta_0/\eta) \propto C^{\alpha/3} \quad (6)$$

where η_0 and η are the luminescence quantum efficiency of Eu^{2+} in the absence and presence of Tb^{3+}, respectively; C is the sum concentration of the Eu^{2+} and Tb^{3+}. Eq.6 with α=6, 8, 10 corresponds to the dipole-dipole, dipole-quadrupole, and quadrupole-quadrupole interactions, respectively. The value of η_0/η can be approximately estimated from the correlated lifetime ratio (τ_{S0}/τ_S), so Eq.6 can be changed as follows

$$(\tau_{S0}/\tau_S) \propto C^{\alpha/3} \quad (7)$$

The relationships of $(\tau_{S0}/\tau_S) \propto C^{\alpha/3}$ are illustrated in Figure 6. For Eu1, by consulting the fitting factor R, the relation $(\tau_{S0}/\tau_S) \propto C^{10/3}$ has the best fitting, implying that the quadrupole-quadrupole interaction is applied for the energy transfer from Eu1 to Tb^{3+}. However, as shown in Figure 6b, the relation $(\tau_{S0}/\tau_S) \propto C^{8/3}$ has the best fitting, the results show that the dipole-quadrupole interaction is applied for the energy transfer from Eu2 to Tb^{3+}. Our previous results show that there may be the energy transfer from Eu2 (500 nm) to Eu1 (418 nm).[32] Therefore, for Eu1 and Eu2, it is reasonable that there is the different mechanism of energy transfer.

3.4 CIE and CCT of $Sr_3La(PO_4)_3$:Eu^{2+}, $y$$Tb^{3+}$ and $Sr_3La(PO_4)_3$:Tb^{3+}

Table 1. Variation of Quantum Efficiency (QE) (λ_{ex}=320 nm), and CIE Chromaticity Coordinate of samples (λ_{ex}=365 nm)

$Sr_3La(PO_4)_3$:0.03Eu^{2+}, yTb^{3+}	CIE (X, Y)	QE (%)
$Sr_3La(PO_4)_3$:0.03Eu^{2+}	(0.1624, 0.1186)	61.7
$Sr_3La(PO_4)_3$:0.07Tb^{3+}	(0.3172, 0.5775)	29.2
y=0.005	(0.1707, 0.1391)	62.3
y=0.01	(0.2044, 0.1879)	65.9
y=0.02	(0.2380, 0.2439)	71.6
y=0.03	(0.3187, 0.3869)	60.9
y=0.05	(0.3511, 0.4475)	56.2
y=0.07	(0.3505, 0.4971)	50.9
y=0.10	(0.3702, 0.5480)	48.1

Table 1 and Figure 7 shows the CIE chromaticity coordinates and luminescence photos of $Sr_3La(PO_4)_3$:0.03Eu^{2+}, $y$$Tb^{3+}$ (y=0-0.10) and $Sr_3La(PO_4)_3$:0.07Tb^{3+}. For $Sr_3La(PO_4)_3$:0.03Eu^{2+}, yTb^{3+} phosphors, as the value of y increases from 0 to 0.10, the photoluminescence color can be easily modulated from blue to yellow-green, and

eventually to green, which is due to the different emission composition of Eu^{2+} and Tb^{3+} ions. The results directly prove the energy transfer from Eu^{2+} to Tb^{3+}, and the emission color can also be tuned by increasing Tb^{3+} concentration. Moreover, we observe that the maximum quantum efficiency can reach 71.6%, which is considered to have potentially tunable phosphor for white LEDs fabrication. From the above results, we can clearly see that the emission of Eu^{2+} and Tb^{3+} ions occurs simultaneously and yields a tunable blue-green light emission as a result of energy transfer.

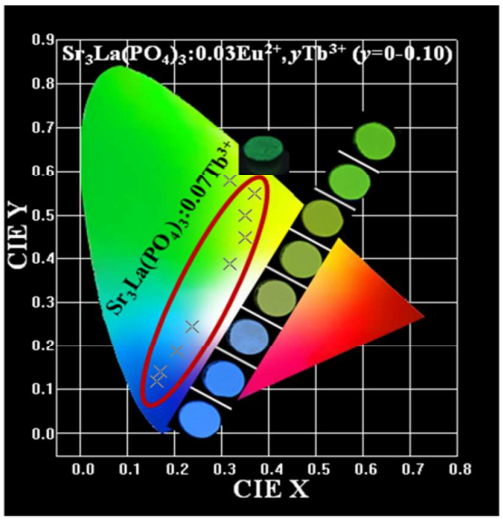

Figure 7. CIE chromaticity coordinates and the corresponding luminescence photograph of $Sr_3La(PO_4)_3$:0.03Eu^{2+}, $y$$Tb^{3+}$ (0-0.10) and $Sr_3La(PO_4)_3$:0.07Tb^{3+} (λ_{ex}=365 nm).

3.5 Thermal quenching properties

For application, the thermal stability of phosphor is one of important issues to be considered. The emission spectra of $Sr_3La(PO_4)_3$:0.03Eu^{2+}, 0.07Tb^{3+} with different temperatures are shown in Figure 8. In order to investigate the temperature dependence of emission intensity, the inset of Figure 8a depicts the temperature quenching characteristics of $Sr_3La(PO_4)_3$:0.03Eu^{2+}, 0.07Tb^{3+} and YAG:Ce^{3+}. The results show that the intensity of sample drops to about 81.0% when temperature is 150 °C, in other words, the sample has a good thermal quenching property.

The activation energy (E_a) can be expressed by[40]

$$\ln(I_0/I)=\ln A-E_a/kT \quad (3)$$

where I_0 and I are luminescence intensity of $Sr_3La(PO_4)_3$:0.03Eu^{2+}, 0.07Tb^{3+} at room temperature and the testing temperature, respectively. A is a constant; k is the Boltzmann constant (8.617×10-5 eV K^{-1}). The fitting result is shown in Figure 8b and the activation energy ΔE is achieved as 0.274 eV. The relatively high activation energy indicates that $Sr_3La(PO_4)_3$:0.03Eu^{2+}, 0.07Tb^{3+} has a good thermal stability.

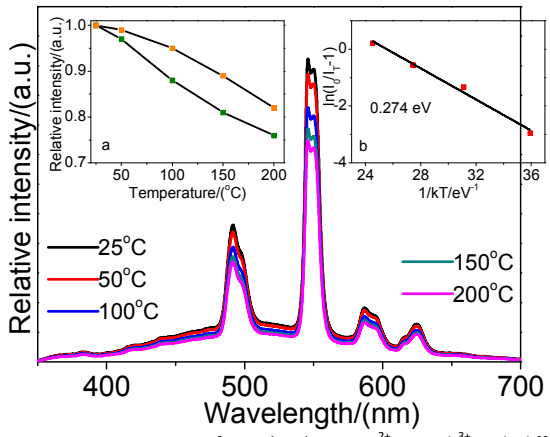

Figure 8. Emission spectra of $Sr_3La(PO_4)_3$:0.03Eu^{2+}, 0.07Tb^{3+} with different temperature (25-200 °C) (λ_{ex}=320 nm).
Inset a: Emission intensity of $Sr_3La(PO_4)_3$:0.03Eu^{2+}, 0.07Tb^{3+} and YAG:Ce^{3+} as a function of temperature (25-250 °C).
Inset b: Arrhenius fitting of emission intensity of $Sr_3La(PO_4)_3$:0.03Eu^{2+}, 0.07Tb^{3+} and the activation energy (ΔE) for thermal quenching.

Conclusions

A series of Eu^{2+} and Tb^{3+} singly-doped and co-doped $Sr_3La(PO_4)_3$ phosphors have been synthesized by the high-temperature solid-state method. Because Eu ions occupy two different Sr^{2+} sites, hence, $Sr_3La(PO_4)_3$:Eu^{2+} shows a strong blue emission around 418 nm and a shoulder locating at 500 nm under ultraviolet excitation. $Sr_3La(PO_4)_3$:Tb^{3+} shows characteristic emission lines of Tb^{3+} under 376 nm excitation. The emission intensities and emission color of $Sr_3La(PO_4)_3$:Eu^{2+}, Tb^{3+} samples can be tuned by the energy transfer from Eu^{2+} to Tb^{3+}, and the energy transfer mechanism can be confirmed to be quadrupole-quadrupole (Eu1) and dipole-quadrupole (Eu2) interaction, respectively. The results can be validated via the agreement of critical distances obtained by the concentration quenching (21.62 Å). These results indicate that the developed phosphor may be potentially tunable emitting phosphor for white LEDs.

Acknowledgements

The work is supported by the National Natural Science Foundation of China (No.50902042), the Funds for Distinguished Young Scientists of Hebei Province, China (No.A2015201129), the Natural Science Foundation of Hebei Province, China (Nos.A2014201035, E2014201037), the Education Office Research Foundation of Hebei Province, China (Nos.ZD2014036, QN2014085), the Midwest Universities Comprehensive Strength Promotion Project.

Notes and references

1. C.-W.Yeh, W.-T. Chen, R.-S. Liu, S.-F. Hu, H.-S. Sheu, J.-M. Chen and H. T. Hintzen. J. Am. Chem. Soc., 2012, 134, 14108-14117.

2. Y. Wang, T. Wen, L. Tang, L. Yang, W. Yang and Y. Zhao. Dalton Trans., 2015, 44, 7578-7585.

3. F. Baur, F. Glocker and T. Jüstel. J. Mater. Chem. C, 2015, 3, 2054-2064.

4. K. Li, X. Liu, Y. Zhang, X. Li, H. Lian and J. Lin. Inorg. Chem., 2015, 54 (1), 323-333.

5. J. Hou, W. Jiang, Y. Fang, F. Huang. J. Mater. Chem. C, 2013, 1, 5892-5898.

6. C. Liu, D. Hou, J. Yan, L. Zhou, X. Kuang, H. Liang, Y. Huang, B. Zhang and Y. Tao. J. Phys. Chem. C, 2014, 118, 3220-3229.

7. X. Zhang and M. Gong. Dalton Trans., 2014, 43, 2465-2472.

8. Z. Xia and R.-S. Liu. J. Phys. Chem. C, 2012, 116, 15604-15609.

9. T. W. Kuo and T. M. Chen. J. Electrochem. Soc., 2010, 157 (6), J216-J220.

10. K. Li, Y. Zhang, X. Li, M. Shang, H. Lian and J. Lin. Dalton Trans., 2015, 44, 4683-4692.

11. M. Jiao, N. Guo, W, Lü, Y. Jia, W. Lv, Q. Zhao, B. Shao and H. You. Inorg. Chem., 2013, 52, 10340-10346.

12. H. Liu, Y. Zhang, L. Liao and Z. Xia. J. Lumin., 2014, 156, 49-54.

13. S. J. Gwak, P. Arunkumar and W. B. Im. J. Phys. Chem. C, 2014, 118, 2686-2692.

14. W. B. Park, S. P. Singh and K.-S. Sohn. J. Am. Chem. Soc. 2014, 136, 2363-2373.

15. Z. Ci, M. Que, Y. Shi, G. Zhu and Y. Wang. Inorg. Chem., 2014, 53, 2195-2199.

16. W.-T. Chen, H.-S. Sheu, R.-S. Liu and J. P. Attfield. J. Am. Chem. Soc., 2012, 134, 8022-8025.

17. Z. Xia, H. Liu, X. Li, C. Liu. Dalton Trans., 2013, 42, 16588-16595.

18. W.-R. Liu, C.-H. Huang, C.-W. Yeh, J.-C. Tsai, Y.-C. Chiu, Y.-T. Yeh and R.-S. Liu. Inorg. Chem., 2012, 51, 9636-9641.

19. C.-H. Huang, T.-S. Chan, W.-R. Liu, D.-Y. Wang, Y.-C. Chiu, Y.-T. Yeh and T.-M. Chen. J. Mater. Chem., 2012, 22, 20210-20216.

20. C.-H. Huang, T.-M. Chen, W.-R. Liu, Y.-C. Chiu, Y.-T. Yeh and S.-M. Jang. ACS Appl. Mater. Interfaces, 2010, 2, 259-264.

21. J. Chen, Y-G. Liu, L. Mei, Z. Wang, M. Fang and Z. Huang. J. Mater. Chem. C, 2015, 3, 5516-5523.

22. P. Li, Z. Wang, Z. Yang and Q. Guo. J. Mater. Chem. C, 2014, 2, 7823-7829.

23. Z. Xia, Y. Zhang, M. S. Molokeev and V. V. Atuchin. J. Phys. Chem. C, 2013, 117, 20847-20854.

24. S. Miao, Z. Xia, J. Zhang and Q. Liu. Inorg. Chem., 2014, 53, 10386-10393.

25. N. Guo, Y. Huang, Y. Jia, W. Lv, Q. Zhao, W. Lü, Z. Xia and H. You. Dalton Trans., 2013, 42, 941-947.

26. Y. Jia, W. Lü, N. Guo, W. Lü, Q. Zhao and H. You. Phys. Chem. Chem. Phys., 2013, 15, 6057-6062.

27. D. Geng, G. Li, M. Shang, D. Yang, Y. Zhang, Z. Cheng and J. Lin. J. Mater. Chem., 2012, 22, 14262-14271.

28. T. Li, P. Li, Z. Wang, S. Xu, Q. Bai and Z. Yang. RSC Adv., 2015, 5, 71735-71742.

29. N. Guo, W. Lü, Y. Jia, W. Lv and Q. Zhao. ChemPhysChem., 2013, 14, 192-197.

30. N. Guo, Y. Jia, W. Lü, W. Lv, Q. Zhao, M. Jiao, B. Shao and H. You. Dalton Trans., 2013, 42, 5649-5654.

31. N. Guo, Y. Huang, M. Yang, Y. Song, Y. Zheng and H. You. Phys. Chem. Chem. Phys., 2011, 13, 15077-15082.

32. P. Li, Z. Wang, Z. Yang and Q. Guo. J. Electrochem. Soc., 2012, 159 (3), H307-H311.

33. Z. Wang, Z. Xia, M. S. Molokeev, V. V. Atuchin and Q. Liu. Dalton Trans., 2014, 43, 16800-16804.

34. C.-H. Huang and T.-M. Chen. J. Phys. Chem. C, 2011, 115, 2349-2355.

35. P. I. Paulose, G. Jose, V. Thomas, N. V. Unnikrishnan and M. K. R. Warrier. J. Phys. Chem. Solids, 2003, 64, 841-846.

36. G. Blasse. Philips Res. Rep., 1969, 24, 131-144.

37. G. Li, D. Geng, M. Shang, C. Peng, Z. Cheng and J. Lin. J. Mater. Chem., 2011, 21, 13334-13344.

38. M. Shang, C. Li and J. Lin. Chem. Soc. Rev., 2014, 43, 1372-1386.

39. D. L. Dexter and J. H. Schulman. J. Chem. Phys., 1954, 22, 1063-1070.

40. P. Dorenbos. J. Phys.: Condens. Matter, 2005, 17, 8103-8111.